

Electronically and Sterically Induced Structural Distortions in Square-Planar d⁸ Complexes

Alessandra Magistrato, Massimo Merlin, Paul S. Pregosin,* and Ursula Rothlisberger*

Laboratory of Inorganic Chemistry, ETH Zentrum, CH-8092 Zürich, Switzerland

Alberto Albinati*

Chemical Pharmacy, University of Milan, I-20131 Milan, Italy

Received June 2, 2000

The solid-state structure of the cationic MeO-Biphep Rh(I) compound [Rh((*S*)-MeO-Biphep)-(P{OMe}₃)₂][BF₄] (**3**) has been determined by X-ray diffraction. The four P-donors deviate markedly from square-planar geometry, with the phosphite ligands P2 and P2' ca. ±0.61(7) Å from the P1–Rh–P1' plane. This distortion resembles that found for PdBr(*p*-NCC₆H₄)-((*S*)-MeO-Biphep) (**1**). Density functional calculations on a series of systematically varied models of **1** reveal three major components to be responsible for the observed distortion from square-planar geometry: (i) attractive aromatic ring π – π interactions, (ii) electronic stabilization of coplanar aromatic rings in pseudo-trans positions, and (iii) P-phenyl and MeO-Biphep-phenyl intraligand repulsive steric interactions. Additional DFT studies on the *p*-tolyl-Binap analogue of **1**, PdBr(*p*-NCC₆H₄)(*R*)-*p*-Tol-Binap) (**2**), explain the source of the extremely long Pd–P2 bond distance, 2.437(1) Å, in **2**. Despite the structural similarity between **1** and **2**, the calculations rationalize the observation of a pronounced distortion from a square-planar geometry in the former that is essentially absent in the latter.

Introduction

Metal complexes with d⁸ electronic configuration routinely demonstrate square-planar geometry.¹ This structural feature is associated with the relative energies of the eight d electrons. When these differences decrease, i.e., when the energy cost involved in pairing the electrons is greater than the ligand field splitting, one observes a tetrahedral structure.² In compounds of the d⁸ centers Pd(II), Pt(II), Rh(I), and Ir(I), increasing the molecular size and decreasing the local symmetry frequently lead to modest distortions from ideal square-planar geometry. Specifically, the presence of bulky cis-phosphines readily leads to an opening of the P–M–P angle.³ In a related way, *trans*-MHL₂ derivatives often demonstrate P–M–P angles much less than 180° due to the small size of the hydride ligand (L = halogen, nitrogen, or phosphine donor).⁴

We have recently shown⁵ that the solid-state structures of the related aryl complexes PdBr(*p*-NCC₆H₄)-((*S*)-MeO-Biphep) (**1**) and PdBr(*p*-NCC₆H₄)(*R*)-*p*-Tol-Binap) (**2**) are quite different. The former shows marked

distortions from a typical local square-planar geometry. Although there is sufficient space for both the aryl and bromide ligands in **1**, these anionic ligands deviate so strongly from the coordination plane defined by the two P-donors and the metal, +0.88 and –0.57 Å, respectively, that one can no longer speak of a square-planar geometry.

Further, although the cis angles P1–Pd–P2 = 94.06(3)°, P2–Pd–Br = 89.69(2)°, and C1L–Pd–Br = 90.09(9)° in **1** are not very distorted, the trans angles, P2–Pd–C1L = 163.02(10)° and P1–Pd–Br = 158.96(3)°, are quite far from 180°. We suggested⁵ that a reasonable description of the distortion involved rotation of the P–Pd–P and C1–Pd–Br planes, relative to one another, and not a tetrahedral distortion. The X-ray data make it clear that crystal-packing forces are not involved.

For the related aryl-Binap complex **2**, the observed coordination geometry is only slightly distorted square planar; however, the Pd–P2 bond length, trans to the aryl, at 2.437(1) Å represents one of the longest Pd–P bonds ever reported. The analogous distance in **1**, Pd–P2, is 2.3501(9) Å.

We report here an extension of our structural studies in which we (i) show that a completely different Rh(I) MeO-Biphep complex can undergo the same type of distortion and (ii) use density functional theory (DFT) to rationalize its origins.

Results

Complex **3** was prepared as shown in Scheme 1.

X-ray Structure of 3. The cationic MeO-Biphep Rh(I) compound [Rh((*S*)-MeO-Biphep)(P{OMe}₃)₂][BF₄] (**3**)

(1) Shriver, D. F.; Atkins, P. W.; Langford, C. H. *Inorganic Chemistry*; Oxford University Press: Oxford, U.K., 1990; p 194.

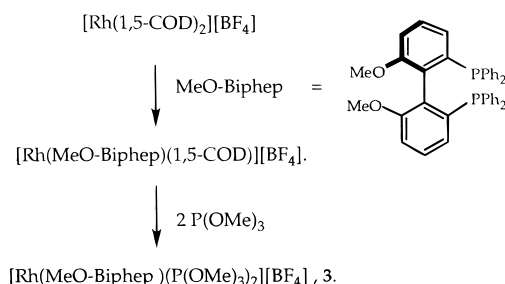
(2) Huheey, J. E. *Inorganic Chemistry*, 3rd ed.; Harper International SI: Cambridge, U.K., 1983; p 411.

(3) Kerr, A.; Mardr, T. B.; Norman, N. C.; Orpen, A. G.; Quayle, M. J.; Rice, C. R.; Timms, P. L.; Whittell, G. R. *Chem. Commun.* **1998**, 319. Porzio, W.; Musco, A.; Immirzi, A. *Inorg. Chem.* **1980**, 19, 2537.

(4) Butts, M. D.; Scott, B. L.; Kubas, G. J. *J. Am. Chem. Soc.* **1996**, 118, 11831–11843 and references therein. For *trans*-PdF(C₆H₅)(PPh₃)₂ the P–Pd–P angle is ca. 174°; see: Fraser, S. L.; Antipin, M. Y.; Khroustalyov, V. N.; Grushin, V. V. *J. Am. Chem. Soc.* **1997**, 119, 4769–4770.

(5) Drago, D.; Pregosin, P. S.; Tschöerner, M.; Albinati, A. *J. Chem. Soc., Dalton Trans.* **1999**, 2279–2280.

Scheme 1

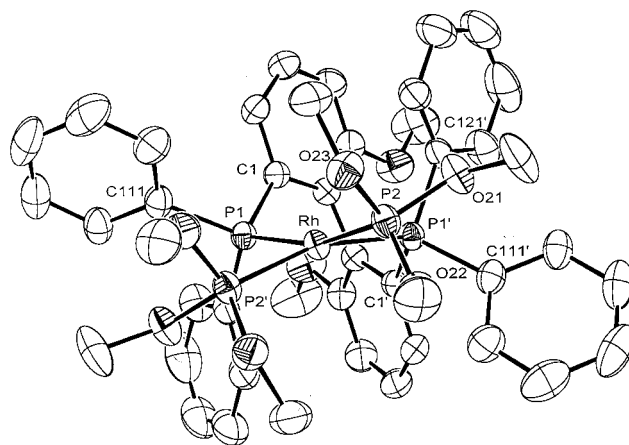

Table 1. Selected Bond Lengths (Å) and Angles (deg) for **3**

Rh–P(2)	2.249(1)	Rh–P(1)	2.335(1)
P(2)–Rh–P(2')	88.07(6)	P(2')–Rh–P(1')	163.97(4)
P(2)–Rh–P(1)	163.97(4)	P(1)–Rh–P(1')	90.63(5)
P(2')–Rh–P(1)	92.86(4)		

contains the MeO-Biphep ligand (P1 and P1') and two trimethyl phosphite donors (P2 and P2'), so that the immediate coordination sphere of the rhodium contains four P-donors. Selected bond lengths and bond angles are given in Table 1. As the molecule lies on a crystallographic C_2 axis, there are only two independent Rh–P separations, Rh–P(1) = 2.335(1) Å and Rh–P(2) = 2.249(1) Å. It is interesting that the phosphite separation is considerably shorter; however, neither of these bond distances is unusual.

The distortion of **3** from square-planar geometry is visible in Figure 1 and can be best described by the deviation of the two phosphite ligands, P2 and P2', $\pm 0.61(7)$ Å from the P1–Rh–P1' plane. Consequently, this rhodium derivative demonstrates a "rotation" similar to that found in the aryl–palladium complex **1** noted above. The cis angles P(2)–Rh–P(2') = 88.07(6)°, P(2)–Rh–P(1) = 92.86(4)°, and P(1)–Rh–P(1') = 90.63(5)° are, again, not far from the expected 90°. On the other hand, the trans angle, P(2)–Rh–P(1) = 163.97(4)°, is considerably smaller than the routine value of 175–180° and is reminiscent of the value P2–Pd–C1L in **1**, 163.0(1)°. The two P-phenyl ipso carbons C111 and C121 are $-0.72(4)$ and $+1.60(9)$ Å below and above the P1–Rh–P1' plane, respectively, in keeping with the tendency of MeO-Biphep complexes to reveal chiral pockets containing pseudoequatorial and pseudoaxial substituents.^{6–8}

Interestingly, the structure of **3** shows π – π stacking of a P-phenyl ring with the backbone of MeO-Biphep. The shortest contact distances⁹ between these facing rings (C121–C126 and C1'–C6') are ca. 3.1–3.4 Å, in agreement with previous observations. We have come to accept this π – π stacking as a characteristic of this type of complexed ligand.^{6–8} A consequence of this π – π stacking is a similar conformation of the four P-phenyl


Figure 1. View of the complex **3** from behind the phosphite ligands looking toward the Pd atom. The two phosphite P-donors are relatively far from the P1–Pd–P1' plane.

rings in complexes of this ligand; i.e., one observes closely related shapes for the (metal)(MeO-Biphep) moiety.

Calculations. Density functional theory¹⁰ provides chemists with a potent computational tool. This is true not only for biochemical¹¹ and classical organic¹² chemistry problems but also increasingly for questions involving metal ions in coordination and organometallic chemistry.^{13–16}

The X-ray structure of the chelating phosphine–aryl complex PdBr(p-NCC₆H₄)((S)-MeO-Biphep) (**1**) reveals an unexpected deviation from "routinely observed" pseudo-square-planar coordination spheres. Specifically, the two trans angles P–Pd–C and P–Pd–Br are relatively small, 163 and 159°, respectively, whereas the Pd–P bond length trans to the aryl carbon, 2.35 Å, is only modest in length. In the hope of understanding the source of these distortions, we carried out DFT calculations on the entire molecule. In addition, to identify specific electronic and steric effects we have constructed a series of model complexes, based on a simplified molecular structure, which allow us to systematically include or exclude the influence of different structural fragments. Therefore, our computational approach is partially "retro-structural". As a reference we begin with an optimization of the full molecule, model 1 (see Figure 2 and Table 2), since a comparison between the calculated and observed solid-state structures provides a measure of the performance of the computational scheme.

Figure 2 and Table 3 show a comparison of the first computational result with that observed experimentally. The table gives selected bond lengths and bond angles

(6) Bolm, C.; Kaufmann, D.; Gessler, S.; Harms, K. *J. Organomet. Chem.* **1995**, 502, 47.

(7) Schmid, R.; Foricher, J.; Cereghetti, M.; Schönholzer, P. *Helv. Chim. Acta* **1991**, 74, 370–389. Schmid, R.; Cereghetti, M.; Heiser, B.; Schönholzer, P.; Hansen, H. *J. Helv. Chim. Acta* **1988**, 71, 897–929.

(8) Tschoerner, M.; Pregosin, P. S.; Albinati, A. *Organometallics* **1999**, 18, 670–678. Trabesinger, G.; Albinati, A.; Feiken, N.; Kunz, R. W.; Pregosin, P. S.; Tschoerner, M. *J. Am. Chem. Soc.* **1997**, 119, 6315. Tschoerner, M.; Trabesinger, G.; Albinati, A.; Pregosin, P. S. *Organometallics* **1997**, 16, 3447. Feiken, N.; Pregosin, P. S.; Trabesinger, G. *Organometallics* **1997**, 16, 5756–5762.

(9) These separations represent the closest contacts from carbon to carbon. The distance from the centers of the two rings is ca. 3.4 Å.

(10) Hohenberg, P.; Kohn, W. *Phys. Rev. B* **1964**, 136, 854. Kohn, W.; Sham, L. J. *Phys. Rev. A* **1965**, 140, 1133.

(11) Carloni, P.; Rothlisberger, U. In *Theoretical Biochemistry Processes and Properties of Biological Systems*; Eriksson, L., Ed.; Elsevier: Amsterdam, in press.

(12) Andzelm, J.; Wimmer, J. E. *J. Chem. Phys.* **1992**, 96, 1280. Rothlisberger, U.; Klein, M. L. *Chem. Phys. Lett.* **1994**, 227, 390.

(13) Ziegler, T. *Density Functional Methods in Chemistry and Material Science*; Wiley: New York, 1997; p 69. Woo, T.; Folga, E.; Ziegler, T. *Organometallics* **1993**, 1289.

(14) Deeth, R. J.; Smith, A.; Hii, K. K.; Brown, J. M. *Tetrahedron Lett.* **1998**, 39, 3229–3232.

(15) Branchadell, V.; Moreno-Manas, M.; Pajuelo, F.; Pleixtas, R. *Organometallics* **1999**, 18, 4934–4941.

(16) Burckhardt, U.; Casty, G. L.; Tilley, T. D.; Woo, T.; Rothlisberger, U. Submitted for publication in *Organometallics*.

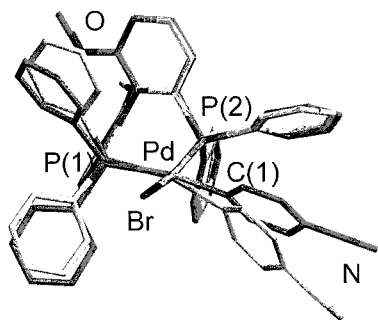


Figure 2. Comparison of the calculated, model 1 (darker gray), and X-ray (lighter gray) structures for **1**.

Table 2. Computational Results for 1

param	X-ray ^a	model 1			
		model 1	constrained	model 2	model 3
Pd–P(1)	2.35	2.39	2.37	2.40	2.42
Pd–P(2)	2.27	2.28	2.29	2.27	2.29
Pd–Br	2.50	2.51	2.50	2.50	2.49
Pd–C(1)	2.10	2.05	2.05	2.03	2.02
P(1)–Pd–C(1)	163.0	169.1	163.5	170.9	176.3
P(2)–Pd–Br	158.9	166.2	160.3	168.4	175.9

^a Standard deviations are <0.01 Å and <0.1° for the distances and angles, respectively.

Table 3. Computational Results for 2

param	X-ray ^a	model 4	model 5	model 6	model 7
Pd–P(1)	2.43	2.43	2.44	2.41	2.45
Pd–P(2)	2.26	2.28	2.28	2.28	2.25
Pd–Br	2.45	2.50	2.50	2.48	2.47
Pd–C(1)	2.03	2.03	2.03	2.02	1.56
P(2)–Pd–C(1)	175.6	173.7	176.7	178.8	174.0
P(1)–Pd–Br	173.5	173.5	174.7	176.9	178.9

^a Standard deviations are <0.01 Å and <0.1° for the distances and angles, respectively.

for the immediate coordination sphere. The primary difference involves the two stacked aromatic ring systems formed by the P-phenyl rings and the MeO-Biphep backbone. As is apparent in Figure 2, the largest deviations occur (i) for one of the P-phenyl rings involved in a π – π -stacking interaction and (ii) for the aryl ligand ring pseudo-trans to it.

Clearly, the attractive π – π interactions have not been described adequately, leading to larger distances between the π – π stacked rings of 3.7 and 4.4 Å, relative to the observed experimental distances between the two sets of parallel rings, 3.6 and 3.7 Å, respectively. Thus, one of the stabilizing stacking interactions has not been reproduced. Since most functionals based on generalized gradient corrections are unable to account for dispersion effects,¹⁷ we do not expect that π – π stacking interactions will be fully described within the DFT approach.

Further, the observation with respect to the aryl ligand and the P-phenyl in a pseudo-trans position (i.e., point ii) represents a significant structural rearrangement. Throughout our calculations, we have noted a strong (electronic) correlation connecting the relative positions of these two fragments (vide infra) which, within the steric restrictions of the environment, seems to maximize the coplanarity of the two aromatic rings. This effect will be discussed below.

The most notable deficiency of model 1 involves the failure to fully reproduce the geometric distortion from

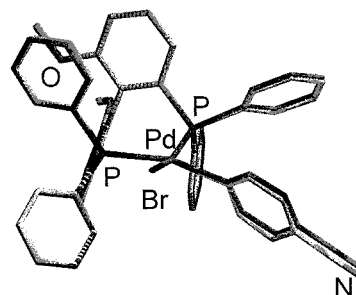


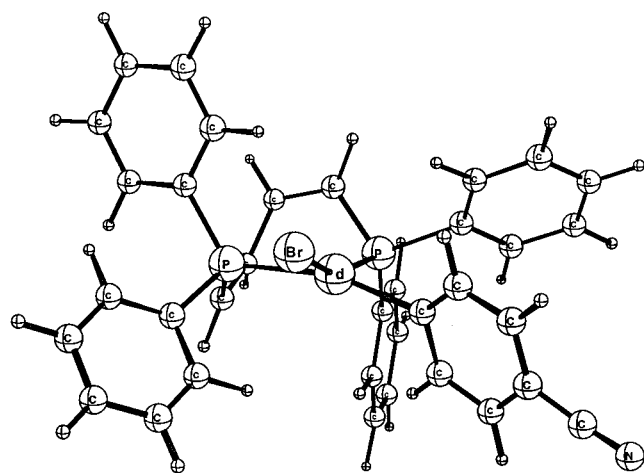
Figure 3. Comparison of the calculated, model 1 constrained, and X-ray structures for **1**. The agreement is so good that one can hardly distinguish between the two.

square-planar geometry. Although significant angular distortions are found, these do not yet approach the observed 17–21° differences found in **1**.

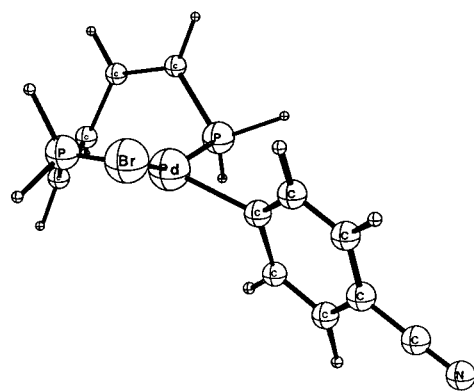
To simulate the effect of the π – π stacking interactions, we performed a second calculation (model 1 constrained) in which the appropriate rings are constrained to the experimentally observed distance and show these results in Figure 3 and Table 3. This a posteriori addition affords a calculated structure in excellent agreement with that observed by X-ray methods. The two structures in Figure 3 are so close that a visual distinction is not obvious. Both the two trans P–Pd–C and P–Pd–Br angles and the Pd–donor atom separations reflect the X-ray data. This result indicates that there are, indeed, attractive π – π interactions present which stabilize a distorted, non-square-planar geometry. From the energy difference between the freely optimized structure and the one in which the geometry optimization was performed with the additional constraint, we estimate that the π – π interactions contribute at least 3.6 kcal/mol to the stabilization of the molecule.

To identify possible further contributors to the observed structural distortions, we systematically simplified the molecule with a view to isolating individual structural features. The model compounds **2** and **3** are shown in Figure 4, and the resulting structural parameters are, again, given in Table 2. In model 2, almost all of the MeO-Biphep backbone has been removed, leaving only the four carbons which, together with the Pd and P-donors, make up the seven-membered chelate ring. This effectively removes any possible π -stacking. The P–C–C–P torsion angle was constrained to that observed in the X-ray results. Apart from a lengthening of the Pd–P(1) bond trans to the aryl donor, these results do not markedly differ from those found for model 1; however, a new subtle effect is noticeable. The aryl ligand ring and one of the P-phenyl rings are rotated into positions which would not have been possible if the backbone were present (e.g., see Figure 5 and the short 1.65 Å contact). By comparing the total energy of model 2 both in its equilibrium geometry and in a second conformation in which the aromatic rings are kept in the original (solid-state) orientation, we estimate that steric restrictions add about 2.3 kcal/mol relative to the energy of the more favorable rotated orientation.

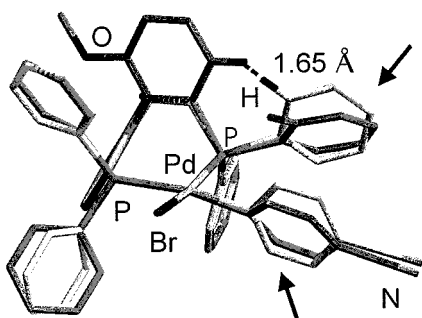
To characterize the effect of the remaining fragments, we have further simplified the structural model by removing the four P-phenyl rings of **1** and replacing them by hydrogen atoms (see model 3). From these



Model 2

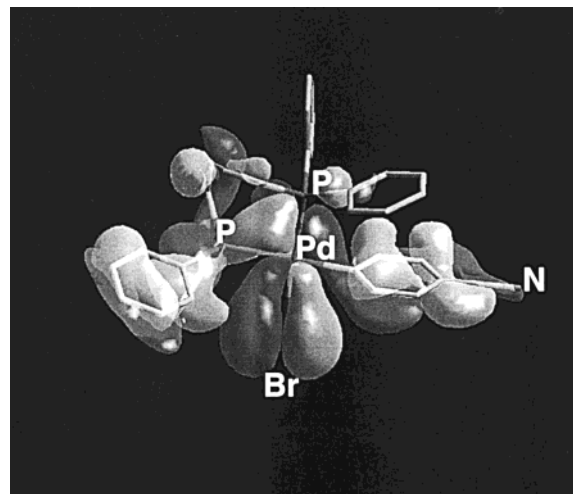


Model 3

Figure 4. The two model ligands used in calculations 2 and 3 (Table 2) and 5 and 6 (Table 3).**Figure 5.** Comparison of the calculated, model 1 (darker gray), and model 2 (lighter gray) structures for **1**. Since the "lighter gray" backbone is absent, the rings can rotate toward the open space.

results we note that the Pd–P(1) bond trans to the aryl donor is longer and approaches known literature values.¹⁸ The angular compression associated with the trans angles, e.g., P(1)–Pd–C(1), has almost vanished, indicating that the phenyl ligands contribute substantially to the overall distortion of the molecule.

As mentioned earlier, there exists a strong correlation involving the positions of the aryl ligand ring and the axial P-phenyl ring in a pseudo-trans position. The

**Figure 6.** HOMO-4 at a contour level of 2.0 atomic units showing a strong correlation involving the positions of the aryl ligand ring and the axial P-phenyl ring in a pseudo-trans position.

molecule tries to attain coplanarity of these two systems with maximal overlap throughout the conjugated system (see Figure 6). This electronic driving force appears to be a further important component in inducing the structural distortion of the square-planar coordination plane. A perfectly coplanar arrangement together with an ideal square-planar coordination geometry leads to the close steric contacts, e.g., as shown in Figure 5, which are only released through a nonplanar coordination geometry and some compromise in coplanarity.

Model 3, in which all the bulky structural fragments have been removed, provides a fully electronically determined reference system. To estimate the energy difference between an ideal square-planar geometry and the distortion found in **1**, we have compared the total energy of model 3 in both its ideal equilibrium structure and in a configuration in which the P–Pd–C and the P–Pd–Br angles have been constrained to the values observed on the crystal structure. This procedure leads to an estimate of the overall (electronic) distortion energy of about 8.9 kcal/mol.

The solid-state structure of the related *p*-Tol-Binap complex PdBr(*p*-NCC₆H₄)((*R*)-*p*-Tol-Binap) (**2**) reveals an extremely long Pd–P(1) bond length, ca. 2.44 Å, for the phosphorus trans to the aryl ligand but little distortion from a classical square-planar structure. To rationalize these observations, three further models, 4–6, were developed. In these (i) the molecule is fully optimized, (ii) the binaphthyl backbone has been removed but, again, the P–C–C–P torsion angle constrained to that observed in the X-ray results (i.e., similar to model 2), and (iii) all four *p*-tolyl rings plus the backbone are deleted (in analogy with model 3). All three calculations (see Table 3) afford good agreement with the X-ray results with respect to the observed Pd–P bond length, ca. 2.44 Å, and the two trans angles, P–Pd–C = 175.6° and P–Pd–Br = 173.6°. In model 5, in which the *p*-Tolyl groups remain, the computational results, 2.44 Å and 176.7° and 174.7°, respectively, are somewhat better than those in model 6, suggesting that the bulky *p*-Tol groups contribute to some modest molecular distortions, e.g., Pd–P bond lengthening.

Binap complex **2** can accommodate both the π – π

(18) Orpen, A. G.; Brammer, L.; Allen, F. H.; Kennard, O.; Watson, D. G.; Taylor, R. *J. Chem. Soc., Dalton Trans.* **1989**, S1–S83.

Table 4. Experimental Data for the X-ray Diffraction Study of [Rh(MeO-Biphep)(P{OMe}₃)₂]BF₄ (3)

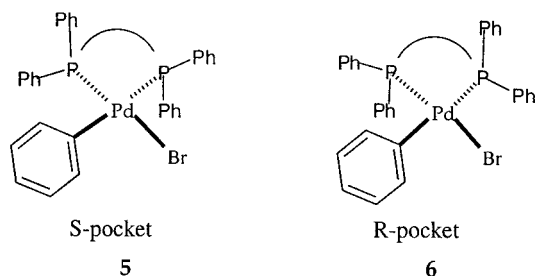
compd	3
formula	C ₄₄ H ₅₀ BF ₄ O ₈ P ₄ Rh
mol wt	1020.44
data collectn <i>T</i> , K	295
diffractometer	Bruker SMART CCD
cryst syst	tetragonal
space group (No.)	<i>P</i> 4 ₂ <i>c</i> (114)
<i>a</i> , Å	11.7811(4)
<i>b</i> , Å	11.7811(4)
<i>c</i> , Å	33.4672(15)
<i>V</i> , Å ³	4645.1(3)
<i>Z</i>	4
ρ_{calcd} , g cm ⁻³	1.459
μ , cm ⁻¹	11.44
radiation	Mo K α (graphite monochrom, $\lambda = 0.710\ 73\ \text{\AA}$)
θ range, deg	1.22 < θ < 29.47
no. of indep data	3499
no. of obsd rflns (<i>n</i> _o ; $ F_o ^2 > 2.0\sigma(F ^2)$)	3078
transmissn coeff	0.65–0.98
no. of params refined (<i>n</i> _r)	272
R1(obsd rflns) ^a	0.040
wR2(obsd rflns) ^b	0.107
GOF ^c	0.966

^a $R1 = \sum(|F_o| - (1/k)F_c)/\sum|F_o|$. ^b $wR2 = [\sum w(F_o^2 - (1/k)F_c^2)^2 / \sum w(F_o^2)^2]$. ^c $GOF = [\sum w(F_o^2 - (1/k)F_c^2)^2 / (n_o - n_r)]^{1/2}$.

stacking interaction of the aromatic rings and the coplanarity of the P-phenyl-ligand aryl fragments without steric problems while simultaneously maintaining an almost ideal square-planar coordination geometry.

Model 7, in Table 3, is based on the hydride complex PdHBr(modified bidentate), in which the bidentate has been reduced in size by, again, eliminating both the backbone and the P-aryl groups. As this is the smallest chelate, the calculated value of ca. 2.45 Å for the Pd–P(1) bond length trans to the hydride represents the electronically controlled upper limit for this parameter.

An additional point surfaces when comparing **1** with **2**. The difference in absolute configuration between the aryl structures of the (*S*)-MeO-Biphep and the (*R*)-Binap complexes leads to a previously unnoticed steric effect. The abbreviated structures **5** and **6** show the chiral



pockets of the two bidentates viewed from behind the Pd–aryl group looking toward the Pd atom. Given that both aryl ligands lie above the P–Pd–P coordination plane (ca. 0.88 and 0.09 Å, respectively), the (*R*)-Binap aryl ligand is positioned closer to the equatorial P-ring, while the (*S*)-MeO-Biphep aryl ligand lies further away from its proximate equatorial P-phenyl. This subtle difference (as yet overlooked in mechanistic discussions involving, e.g., the enantioselective Heck Reaction) can also contribute to the relative stability of these two chiral aryl Pd complexes.

Discussion

Noncovalent π – π stacking interactions between pseudo-parallel aromatic rings have been the subject of considerable discussion. They have been considered as information vectors, which can define and rule self-assembly processes¹⁹ and which, as some authors suggest, might be the result of π – σ attractions which overcome π – π repulsions.²⁰ Barriers to rotation seem to depend on the nature of the ring substituents,²¹ with an increasing number of electron-withdrawing groups on one ring affording a higher barrier. Phosphine-phenyl to substrate-phenyl stacking has been observed in homogeneous hydroformylation²² and allylic alkylation.^{23,24} Studies on intermediates in the latter chemistry have suggested a weakening of one end of a palladium π -allyl complex.^{23,25} There are also reports in which the stacking arises from crystal packing²⁶ and a report connecting this feature to nonlinear optical properties.²⁷

There is no contradiction in suggesting that π – π stacking interactions can be both attractive and repulsive, provided that the ring–ring separations are not ignored. At distances in excess of 4 Å attractive forces may be operating, whereas, once the rings are compressed to <3.4 Å, steric repulsion plays an important role. For **1** (and presumably **3** as well) our computational results suggest that the MeO-Biphep backbone (containing a methoxy donor) and a P-phenyl ring (with its phosphonium-like P atom) prefer π – π stacking, which in turn contributes to the molecular distortion. For **2**, the Binap ligand readily accommodates the three features: π – π interactions, quasi coplanarity of the aryl ligand, and the axial P-phenyl in pseudo-trans position and square-planar geometry. Partially, this is achieved by lengthening the Pd–P bond trans to the aryl.²⁸

We conclude that the combined effects of π – π stacking interactions and electronically favorable coplanar arrangements of aromatic rings together with P-phenyl–aryl and P-phenyl–MeO-Biphep repulsive steric interactions are responsible for the observed distortion from square-planar geometry in the aryl complex PdBr-(*p*-NCC₆H₄)(MeO-Biphep). Given that reports on metal

(19) Claessens, C. G.; Stoddard, J. F. *J. Phys. Org. Chem.* **1997**, *10*, 254–272.

(20) Hunter, C. A.; Sanders, M. J. K. *J. Am. Chem. Soc.* **1990**, *112*, 5525–5534.

(21) Cozzi, F.; Ponzini, F.; Annunziata, R.; Cinquini, M.; Siegel, J. S. *Angew. Chem.* **1995**, *107*, 1092–1094.

(22) Castonguay, L. A.; Rappe, A. K.; Casewit, C. J. *J. Am. Chem. Soc.* **1991**, *113*, 7177–7183.

(23) Abbenhuis, H. C. L.; Burckhardt, U.; Gramlich, V.; Köllner, C.; Pregosin, P. S.; Salzmann, R.; Togni, A. *Organometallics* **1995**, *14*, 759–766.

(24) Barbaro, P.; Pregosin, P. S.; Salzmann, R.; Albinati, A.; Kunz, R. W. *Organometallics* **1995**, *14*, 5150.

(25) Pregosin, P. S.; Trabesinger, G. *J. Chem. Soc., Dalton Trans.* **1998**, 727–734. Pregosin, P. S.; Salzmann, R. *Coord. Chem. Rev.* **1996**, *155*, 35.

(26) Geremia, S.; Randaccio, L.; Mestroni, G.; Milani, B. *J. Chem. Soc., Dalton Trans.* **1992**, 2117–2118.

(27) Bahl, A.; Grahn, W.; Stadler, S.; Feiner, F.; Bourhill, G.; Bräuchle, C.; Reisner, A.; Jones, P. G. *Angew. Chem.* **1995**, *107*, 1587.

(28) Although the Pd–P bond length of ca. 2.45 Å may represent an electronically controlled upper limit, a separation of ca. 2.51 Å with P trans to an SiCl₃ ligand has recently been recorded. This separation is thought to contain a strong steric contribution to this very long bond length. See: Woo, T. K.; Pioda, G.; Röthlisberger, U.; Togni, A. Chiral Pd(II)-Bis(Trichlorosilyl) Complexes. Synthesis, Structure, and Combined QM/MM Computational Studies. *Organometallics* **2000**, *19*, 2144–2152.

complexes with relatively large complex chiral auxiliaries are increasing, and that the observation of π - π stacking is a relatively frequent occurrence, it is likely that additional markedly distorted coordination compounds will appear.

Experimental Section

Crystallography. Dark yellow crystals of $[\text{Rh}(\text{MeO-Biphep})(\text{P}(\text{OMe})_3)_2]\text{BF}_4$ (**3**) were obtained from CH_2Cl_2 /diethyl ether solution and are air stable.

For the data collection, a prismatic single crystal was mounted on a Bruker SMART CCD diffractometer. The space group was determined from the systematic absences, while the cell constants were refined at the end of the data collection with the data reduction software SAINT.²⁹ Data were collected by using an ω scan in steps of 0.3° . The collected intensities were corrected for Lorentz and polarization factors²⁹ and empirically for absorption using the SADABS program.³⁰

Selected crystallographic and other relevant data are listed in Table 1 and in Supplementary Table S1 (Supporting Information). The standard deviations on intensities were calculated in term of statistics alone, while those on F_o^2 were calculated as shown in Table 4. The structure was solved by direct and Fourier methods. Both the Rh and B atoms lie on a crystallographic C_2 axis, and therefore only half of the molecule is independent. The data were refined by full-matrix least squares,³¹ minimizing the function $\sum w(F_o^2 - (1/k)F_c^2)^2$. The BF_4^- moiety was found to be disordered, as can be seen by the high values of the displacement parameters; thus, the resulting geometry for the anion is not accurate. During the refinement anisotropic displacement parameters were used for all atoms, except for the F atoms, which were treated isotropically. No extinction correction was deemed necessary. Upon convergence (see Supplementary Table S1) the final difference Fourier map showed no significant peaks. The contribution of the hydrogen atoms, in their calculated position ($\text{C-H} = 0.95$ Å), $B(\text{H}) = 1.5[B(\text{C}_{\text{bonded}})(\text{\AA}^2)]$, was included in the refinement using a riding model. Refining the Flack parameter³² tested the handedness of the structure.

All calculations were carried out by using the PC version of the SHELX-97 programs.³¹ The scattering factors used, corrected for the real and imaginary parts of the anomalous dispersion, were taken from the literature.³³

Computations. All reported DFT calculations were performed using the Amsterdam density functional (ADF) program.³⁴ The electronic configurations of the molecular systems were described by a triple-STO basis set on the transition-metal center for the ns , np , nd , $(n+1)s$ and $(n+1)p$ valence shells, whereas a double-STO basis set was used for Br (4s,

4p), P (3s, 3p), C (2s, 2p), N (2s, 2p), O (2s, 2p), and H (1s). The inner shells of the atoms were treated within the frozen core approximation. Energy differences were calculated including Becke's nonlocal exchange³⁵ and Perdew's nonlocal correlation corrections.³⁶ First-order scalar relativistic corrections³⁷ were added to the total energy for the palladium atom. A spin-restricted formalism was used for all the calculations.

$[\text{Rh}(\text{MeO-Biphep})(1,5\text{-COD})][\text{BF}_4]$. To a solution of $[\text{Rh}(1,5\text{-COD})_2][\text{BF}_4]$ (20.3 mg, 0.05 mmol) in dichloromethane (5 mL) was added a solution of the MeO-Biphep ligand (29.1 mg, 0.05 mmol) in dichloromethane (5 mL). After 1 h of stirring the solvent was distilled and the crude red solid complex washed two times with diethyl ether to remove the 1,5-COD. NMR data for the complex in CD_2Cl_2 at 250 MHz: ^{31}P , δ 24.0 (d, $^1J_{\text{P-Rh}} = 145$ Hz); ^1H , δ 6.4–7.8 (m, 26 H, arom), 4.5, 4.8 (two multiplets each of integral 2 H, olefin), 3.35 ppm (s, 6 H, MeO), 2.1, 2.6 (2×2 m, 8 H, 4 CH_2). Anal. Calcd for $\text{C}_{46}\text{H}_{44}\text{O}_2\text{-BF}_4\text{P}_2\text{Rh}$ (880.5): C, 62.75; H, 5.04. Found: C, 61.93; H, 5.37.

$[\text{Rh}(\text{MeO-Biphep})(\text{P}(\text{OMe})_3)_2][\text{BF}_4]$ (3**).** To a dark red solution of $[(\text{MeO-Biphep})\text{Rh}(1,5\text{-COD})][\text{BF}_4]$ (20 mg, 0.023 mmol) in dichloromethane (3 mL) was added 2 equiv of $\text{P}(\text{OMe})_3$ (5.6 mg, 0.045 mmol) in dichloromethane (5 mL). The solution color changes immediately to orange. After it was stirred for 1 h, the solution was concentrated and the final complex **3** precipitated by addition of diethyl ether. Crystals suitable for X-ray diffraction were obtained from CH_2Cl_2 /diethyl ether solution. NMR (CD_2Cl_2 , 250 MHz; spin system AA'XX'M): ^{31}P , δ 124 ($^2J_{\text{P-P}}(\text{cis}) = -45$ Hz, $^2J_{\text{P-P}}(\text{cis}') = -42$ Hz, $^2J_{\text{P-P}}(\text{trans}) = 440$ Hz, $^1J_{\text{Rh-P}} = 224$ Hz); 28 ($^2J_{\text{P-P}}(\text{cis}) = 75$ Hz, $^2J_{\text{P-P}}(\text{cis}') = -45$ Hz, $^2J_{\text{P-P}}(\text{trans}) = 440$ Hz, $^1J_{\text{Rh-P}} = 130$ Hz); ^1H , δ 6.2–7.8 (m, 26 H, arom), 3.39 (m, 18 H, $\text{P}(\text{OMe})_3$), 3.30 (s, 6 H, MeO). Electronic absorption spectra for **3**: 410 nm ($\epsilon = 3383 \text{ M}^{-1} \text{ cm}^{-1}$), 334 ($\epsilon = 6222 \text{ M}^{-1} \text{ cm}^{-1}$), 306 nm ($\epsilon = 8750 \text{ M}^{-1} \text{ cm}^{-1}$) in CH_2Cl_2 . Anal. Calcd for $\text{C}_{44}\text{H}_{50}\text{O}_8\text{BF}_4\text{P}_4\text{Rh}$ (880.5): C, 51.79; H, 4.94. Found: C, 51.41; H, 5.20.

Acknowledgment. P.S.P. and U.R. thank the Swiss National Science Foundation and the ETH Zurich for financial support. A.A. thanks MURST for a research grant. P.S.P. also thanks F. Hoffmann-La Roche AG, Basel, Switzerland, for the gift of the MeO-Biphep bidentate ligand as well as Johnson Matthey for the loan of precious metal salts.

Supporting Information Available: Text giving experimental details and a full listing of crystallographic data for compound **3**, including tables of positional and isotropic equivalent displacement parameters, calculated positions of the hydrogen atoms, anisotropic displacement parameters, and bond distances and angles, as well as an ORTEP figure showing the full numbering scheme. This material is available free of charge via the Internet at <http://pubs.acs.org>.

OM000466Q

(29) SAINT: SAX Area Detector Integration; Siemens Analytical Instrumentation, Madison, WI, 1996.

(30) Sheldrick, G. M. SADABS; Universität Göttingen, Göttingen, Germany, to be published.

(31) Sheldrick, G. M. SHELX-97: Structure Solution and Refinement Package; Universität Göttingen, Göttingen, Germany, 1997.

(32) Flack, H. D. *Acta Crystallogr.* **1983**, A39, 876.

(33) *International Tables for X-ray Crystallography*; Wilson, A. J. C., Ed.; Kluwer Academic: Dordrecht, The Netherlands, 1992; Vol. C.

(34) (a) Baerends, E. J.; Ellis, D. E.; Ros, P. *Chem. Phys.* **1973**, 2, 41. (b) te Velde, G.; Baerends, E. J. *J. Comput. Phys.* **1992**, 99, 84.

(35) Becke, A. *Phys. Rev. A* **1988**, 38, 3098.

(36) Perdew, J. P.; Zunger, A. *Phys. Chem. Rev. B* **1981**, 23, 5048.

(37) (a) Snijeders, J. G.; Baerends, E. J. *J. Mol. Phys.* **1978**, 36, 1789. (b) Snijeders, J. G.; Baerends, E. J.; Ros, P. *Mol. Phys.* **1979**, 38, 1909.